CUMULATIVE DAMAGE OF HIGH-RISE BUILDINGS DURING THE IN-SERVICE PERIOD IN OSAKA, JAPAN

Takeshi Morii[1], Yasuhiro Hayashi[2], Yoshiaki Kumagai[3] and Yoshihiro Ohnishi[4]

[1] *Assist. Prof., Dept. of Architecture and Architectural Eng., Kyoto Univ., Kyoto, Japan*
[2] *Professor, Dept. of Architecture and Architectural Eng., Kyoto Univ., Kyoto,Japan*
[3] *Obayashi Corporation, Tokyo, Japan*
[4] *Geo-Research Institute, Osaka, Japan*
Email: morii@archi.kyoto-u.ac.jp, hayashi@archi.kyoto-u.ac.jp, kumagai.yoshiaki@obayashi.co.jp, onishi@geor.or.jp

ABSTRACT :

The objective of the research is to characterize the remaining performance of existing buildings in terms of the cumulative damage, such as the cumulative plastic ductility and cumulative residual deformation, of the buildings during the in-service period. We performed the response analysis using simulated ground motion records for the scenario earthquakes and/or observed ground motions records. Analysis models are practical models for the high-rise buildings. The cumulative damage of each building is evaluated from the result of the analyses. Our conclusions are; 1) the characteristics of input motions and building responses can be adequately categorized by using a concept of impulse index corresponding to the ratio of the maximum instantaneous input energy to total input energy. 2) the cumulative residual drift and plastic displacement during the in-service period is not so large, whereas the maximum shear story drift angle may equal or larger than 0.02.

KEYWORDS: Cumulative damage, In-service period, Nonlinear response analysis, Impulse index

1. INTRODUCTION

Many buildings in the Kansai region was subjected to severe damage during the 1995 Hyogo-ken Nanbu Earthquake in Kobe. Therefore, there might be many buildings that have potential damage without being repaired. On the other hand, the Earthquake Research Committee in Japan evaluates the probability of the potential of earthquakes (location, magnitude, probability of occurrence) on major active faults and subduction zones. According to the report, the occurrence probability of the Tonankai and Nankai earthquake is more than 50% within the next 30 years from present[1]. Ground motion simulations and observed ground motions strongly indicate that a long-period ground motion, especially of around 5 second components, would be amplified by the deep sedimentary structure in Osaka basin during the earthquakes. Since this period is close to the natural period of high-rise buildings in the basin, there is a probability of severe damage to those structures. Additionally, the seismicity of inland earthquakes will increase before and after the Tonankai and Nankai earthquakes as well as after shocks of the earthquakes. This means, existing or newly built super-high-rise buildings may experience many severe shaking and their damage will be accumulated during its in-service period as shown in Figure 1.

The objective of this research is to clarify the remaining performance of existing buildings and required performance for newly-built super-high-rise buildings in terms of the cumulative damage, such as the cumulative plastic deformation and cumulative residual deformation, of the buildings during the in-service period. Target buildings are super-high-rise buildings with/without hysteretic dampers, and super-high-rise base-isolated buildings in Osaka basin. Simulated ground motions for the scenario earthquakes and/or observed ground motions are used to perform earthquake response analyses. The cumulative damage of each building is evaluated from the result of the analyses.

2. IMPULSE INDEX

The energy input $E_i(t)$ to a linear SDF system, whose natural period is T, is equal to the summation of the kinetic energy $E_k(t)$, energy dissipated in viscous damping $E_d(t)$, and strain energy $E_s(t)$.

$$E_k(t) + E_d(t) + E_s(t) = E_i(t) \tag{2.1}$$

The total input energy E_t and maximum instantaneous input energy ΔE_t during the excitation are expressed as follows.

$$E_t = E_i(\infty) \tag{2.2}$$

$$\Delta E_t = \max_t \{E_i(t) - E_i(t-T)\} \tag{2.3}$$

The total input energy spectra and maximum instantaneous input energy specatra are described from equation (2.2),(2.3) as follows.

$$V_t = \sqrt{2E_t}\,, \quad V_i = \sqrt{2\Delta E_t} \tag{2.4}$$

Using these two energy spectra, an impulse index of input motion can be defined by

$$R_{v(T_1-T_2)} = \int_{T_1}^{T_2} R_v(\tau)d\tau/(T_2 - T_1)\,, \tag{2.5}$$

where $R_v(T)$ is the square root of the ratio of ΔE_t to E_t as

$$R_v(T) = \sqrt{\Delta E_t(T)/E_t(T)}\,. \tag{2.6}$$

If $R_v(T) = 1$, $E_t(T) = \Delta E_t(T)$, implying that the total input energy is energy input during a time interval of natural period T. Therefore, as the input motion becomes impulsive, $R_v(T)$ approaches to 1.0. Contrarily, $R_v(T)$ decreases as the duration time increase. However, total input energy is not monotone increasing necessarily, decreasing in some situations, such as a shown in Figure 2. Figure 2 shows time history of total input energy E_t and maximum instantaneous input energy ΔE_t (natural period T=3s) during 1995 Hyogo-ken Nanbu Earthquake at Fukiai station. Instananeous input energy per natural period become negative value, instananeous input energy is larger than total input energy, so $R_v(T)$ exceeds 1.0. In this study, characteristics of ground motion are characterized by using average R_v between 1 to 5 seconds ($R_{v(1\text{-}5)}$) in natural period (Eqn. (2.5)).

Figure 4 shows the relationship between the impulse index and epicentral distance x for the observed ground motions during the 1995 Hyogo-ken Nanbu Earthquake and the 2004 Tokaido Earthquake occurred at 23:57 September 5. Figure 3 shows the locations of the seismic stations around Osaka area and epicenter of two earthquakes. In the case of the 2004 Tokaido earthquake, if the epicentral distance x<150km, approximately ranges 0.65 to 0.9. If 150km<x, gradually decreases with x as the duration time increases. On the other hands, in the case of the 1995 Hyogo-ken Nanbu earthquake, if the epicentral distance x<100km, approximately ranges 0.7 to 1.0. Particularly, clear dip of $R_{v(1\text{-}5)}$ is shown in about 0.6 and around 200<x<250km in the 2004 Tokaido Earthquake, about 0.7 and around 40<x<60km in the 1995 Hyogo-ken Nanbu Earthquake. This tendency is due to the amplification effects by the deep sedimentary structure in Osaka basin such as a shown in Figure 4.

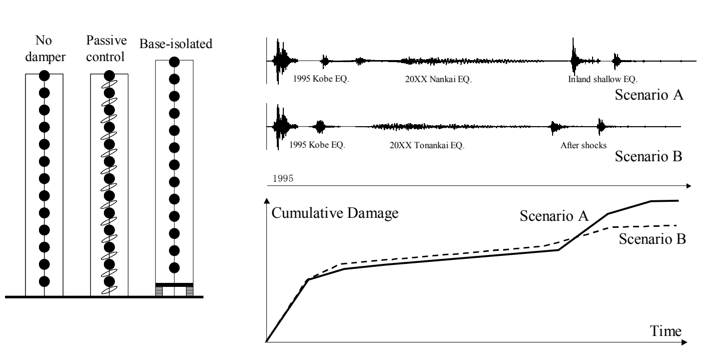

Fig.1 Earthquake occurrence scenario and cumulative damage during the in-service period

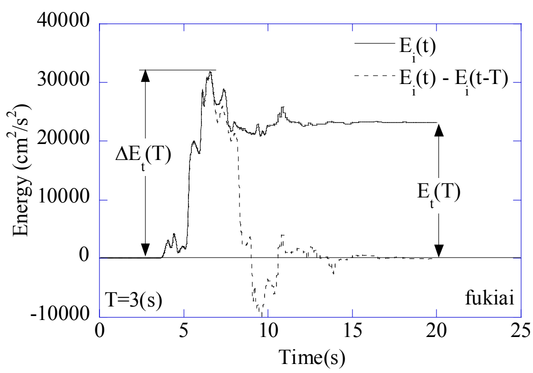

Fig.2 Time-history of the total input energy and instantaneous input energy

Finally, Figure 5 shows the relationship between the impulse index $R_{v(1\text{-}5)}$ and the duration T_d[2] of observed ground motion during two earthquakes. It is conformed the impulse index $R_{v(1\text{-}5)}$ decreases as the duration increase from observation records, duration of ground motion is evaluated by impulse index $R_{v(1\text{-}5)}$ in Kansai region.

3. ANALYSIS MODELS

3.1 Input ground motions

Representative observed ground motions, estimated motions for scenario earthquakes, which will occur in the near future, and design motions are adopted for the input motion of response analyses. Table 1 shows the list of input motions used in the analyses[3], [4], [5], [6]. Figure 6(a),(b) shows the $R_v(T)$ spectra of the input motions in a comparison of the shallow inland earthquakes by active faults (Active Fault (AF) type) and earthquakes near the plate boundary (Plate Boundary (PB) type). Generally, impulse index spectra $R_v(T)$ slightly increases with natural period T, but is almost constant. Therefore, is equivalent to as shown in Fig.6(c). Characterisitcs of ground motions can be sophisticatedly distinguished by as shown in Fig.6(c); if $R_{v(1\text{-}5)}$ >0.8, it is AF type and if $R_{v(1\text{-}5)}$ <0.8, it is PB type.

Table 1 List of input ground motions

Input Motion	Source	Dir.	PGA (cm/s^2)	PGV (cm/s)	PGA/PGV (1/s)	$R_{v(1\text{-}5)}$	Type EQ
El centro	1940 Imperial Valley	NS	511	50	10.2	0.90	AF
Taft	!952 Kern County	EW	497	50	9.9	0.84	AF
Hachinohe	1968 Tokachioki	NS	329	50	6.6	0.78	PB
Kokuji	Building Standard Law, 2000	-	354	46	7.7	0.65	DM
H1	Osaka city[3]	-	210	50	4.2	0.81	AF
H2		-	262	72	3.6	0.83	AF
L1		-	219	47	4.7	0.78	AF
L2		-	259	67	3.9	0.80	AF
Fukiai	1995 Hyogo-ken Nanbu	N37W	802	129	6.2	1.00	AF
JMA Kobe		NS	818	86	9.5	0.99	AF
TCU074	1999 Taiwan	EW	586	73	8.0	0.91	AF
TCU084		EW	989	114	8.7	0.89	AF
TCU068		EW	502	202	2.5	0.92	AF
TTRH02 (Hino)	2000 Western Tottori	NS	927	112	8.3	1.00	AF
HRS014 (Ohno)	2001 Geiyo	EW	441	32	14.0	0.94	IP
JMA Wakuya	2003 Miyagi Hokubu	EW	513	42	12.3	1.03	AF
MYG011 (Ojika)	2003 Off Miyagi	EW	1112	35	32.1	1.11	IP
HKD086 (Chokubetsu)	2003 Off Tokachioki	EW	785	156	5.0	0.77	PB
IBUH03 (Asshi)		EW	377	84	4.5	0.72	PB
TKCH07 (Toyohoro)		EW	404	71	5.7	0.77	PB
JMA Kawaguchi	2004 Mid Niigata Prefecture	EW	1666	134	12.4	1.01	AF
JMA Yamakoshi		EW	714	89	8.0	0.91	AF
NIG019 (Ojiya)		EW	1309	134	9.7	0.97	AF
FKO006 (Fukuoka)	2005 Fukuoka	NS	277	57	4.8	0.93	AF
JMA Wajima	2007 Noto Hanto	NS	439	79	5.5	0.83	AF

No.	Input Motion	Source	Dir.	PGA (cm/s^2)	PGV (cm/s)	PGA/PGV (1/s)	$R_{v(1\text{-}5)}$	Type EQ
26	Nig018 (Kashiwazaki)	2007 Niigataken Chuetsu-oki	NS	667	124	5.4	0.93	AF
27	Kariwa		NS	461	122	3.8	0.86	AF
28	FKS	Estimated earthquake motions (Nankai earthquake)[4]	EW	135	31	4.3	0.64	PB
29	OSKH02		EW	141	35	4.0	0.60	PB
30	YAE		EW	166	33	5.0	0.64	PB
31	FKS	Estimated earthquake motions (Tonankai earthquake)[4]	EW	124	27	4.5	0.69	PB
32	OSKH02		EW	138	39	3.5	0.62	PB
33	YAE		EW	216	54	4.0	0.68	PB
34	FKS	Estimated earthquake motions (Nankai + Tonankai earthquake)[4]	EW	149	36	4.2	0.66	PB
35	OSKH02		EW	159	48	3.3	0.61	PB
36	YAE		EW	319	74	4.3	0.69	PB
37	UF414	Estimated earthquake motions (Uemachi fault) Osaka City[3]	EW	393	94	4.2	0.81	AF
38	UF422		NS	524	144	3.6	0.83	AF
39	UF404		EW	243	52	4.7	0.78	AF
40	CEOR09	Estimated earthquake motions (Uemachi fault) Active Fault Research Center Geological Survey of Japan[5]	EW	232	65	3.6	0.86	AF
41	JMAE8F		EW	765	156	4.9	1.01	AF
42	JMAEBC		EW	815	128	6.4	0.98	AF
43	OSK005		EW	634	111	5.7	0.99	AF
44	KnkIkw		EW	659	175	3.8	0.96	AF
45	CEOR09	Estimated earthquake motions (Uemachi fault) The Central Disaster Prevention Council[6]	EW	359	44	8.1	0.99	AF
46	JMAE8F		EW	656	85	7.7	0.94	AF
47	JMAEBC		EW	542	108	5.0	0.92	AF
48	OSK005		EW	582	70	8.3	0.93	AF
49	KnkIkw		EW	620	97	6.4	0.94	AF

AF: Active Faults Type, PB: Plate Boundary Type, IP: Inner Plate Type, DM: Design Motions

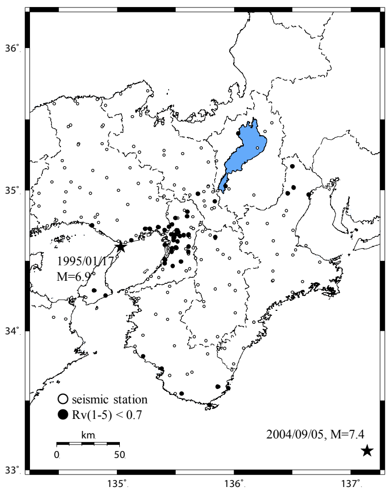

Fig.3 Location of the seismic stations in Kansai region, Japan

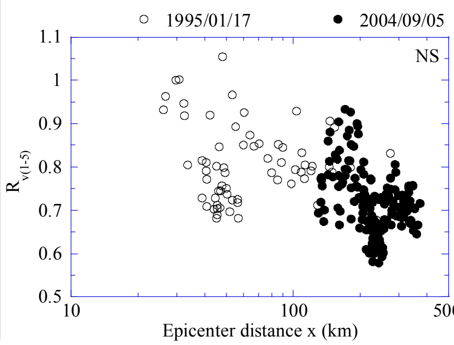

Fig.4 Variations of $R_{v(1\text{-}5)}$ with epicentral distance x

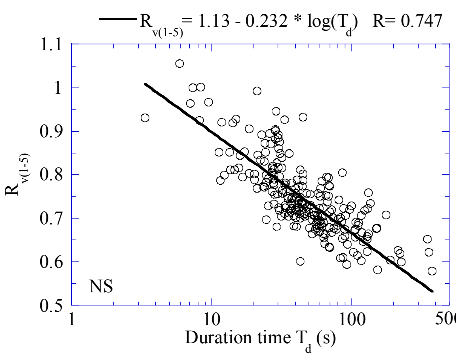

Fig.5 Relationship between duration time T_d and impulse index $R_{v(1\text{-}5)}$

3.2 Analysis Buildings model

Three analysis models of high-rise buildings are used in this paper. These models are developed by slightly modifying those used in the practical design of existing buildings in Osaka.

(a) S40D: 40-story steel building with hysteretic dampers
(b) RC40I: 40-story base-isolated RC building
(c) SRC30: Relatively old 30-story SRC building

Outline of analytical models are shown in Table 2. Restoring force characteristics for three models are shown in Figure 7.

4. RESULTS OF RESPONSE ANALYSES

Nonlinear response analyses are performed by adding zero values to input motions in order to evaluate residual displacement. Figures 8, 9, 10 indicates the maximum shear drift angles R_{max}, cumulative response ductility η, and residual shear drift angles R_r of frame structures. Figure 11 shows the maximum response of base-isolation device.

The followings can be pointed out from these figures.

a) The maximum shear story drift angles R_{max} for $R_{v(1\text{-}5)}$<0.8 is larger than those for $R_{v(1\text{-}5)}$>0.8, if PGV values are specified. This tendency is consistent in the three buildings.

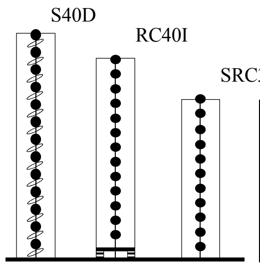

Table 2 Analytical Model

Model	Structure		No. of Story	Hight (m)	Weight (kN)	Natural period (s) 1st	Natural period (s) 2nd
S40D	S	Hysteretic dampers	40	181	986,370	5.4	2.0
RC40I	RC	Base isolation	40	138	432,180	5.0 (2.8)	1.7 (1.1)
SRC30	SRC	-	30	90	309,288	2.1	0.8

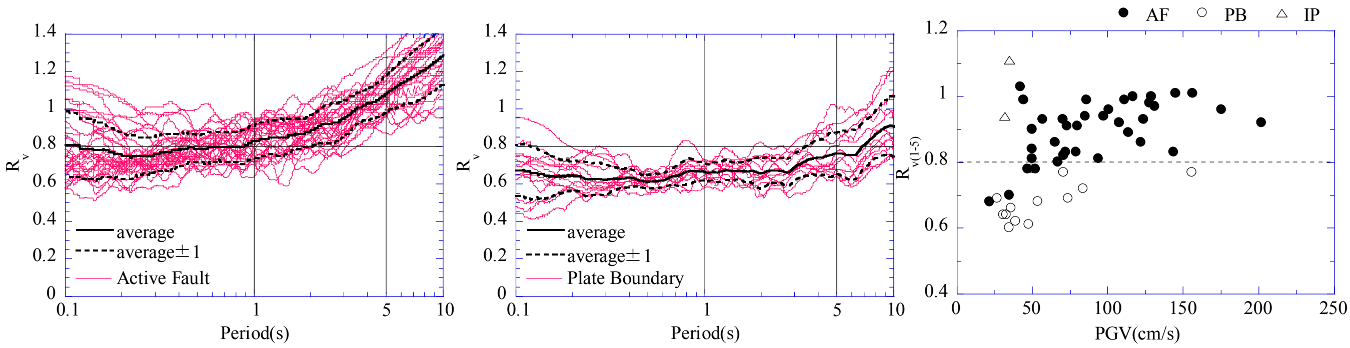

(a) R_v spectra (Active Faults type) (b) R_v spectra (Plate Boundary type) (c) PGV and $R_{v(1\text{-}5)}$

Fig.6 Characteristics of input ground motions

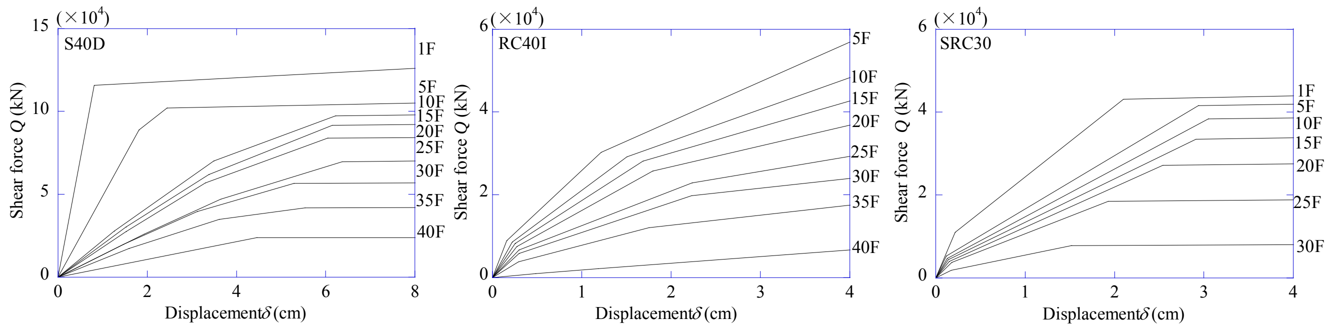

(a) S40D (b) RC40I (c) SRC30

Fig.7 Restoring force characteristics

b) The R_{max} of super-high-rise base-isolated building (RC40I) is relatively small compared with the other two buildings. However, for ground motions with large long-period component generated by inland shallow earthquakes such as 1999 Taiwan earthquake or presumed motions (UF422) for Uemachi fault, the maximum drift δ_{max} of base-isolation devices may be greater than 60cm. On the other hand, the η of base-isolation devices for $R_{v(1\text{-}5)}$ <0.8 may be much larger than those for $R_{v(1\text{-}5)}$ >0.8. However, the residual displacement of the devices is not so large without relation to that accumulation effect during its life-span is not so influential.

c) The η and R_r for SRC30 and RC40I are considered to be too small. We had better revise the restoring characteristics used in the practical design because calculated R_{max} is too large to apply them.

5.CUMULATIVE DAMAGE OF BUILDINGS IN-SERVICE PERIOD

To demonstrate the cumulative damage of the S40D during the in-service period, we assume the earthquake occurrence scenario as shown in Table 3. Namely, the 1995 Kobe earthquake, the Nankai, Tonankai, Nankai+Tonankai earthquake and an inland shallow earthquake occur during the in-service period.

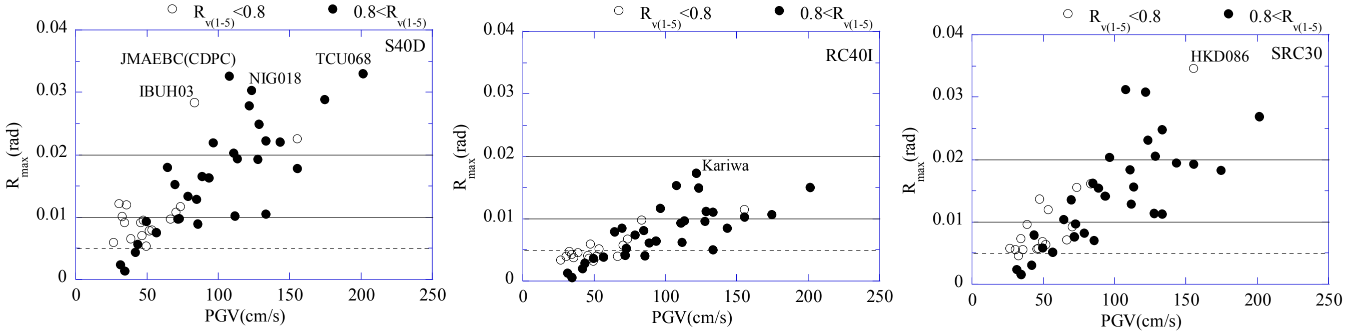

(a) S40D (b) RC40I (c) SRC30

Fig.8 Maximum shear story drift angle

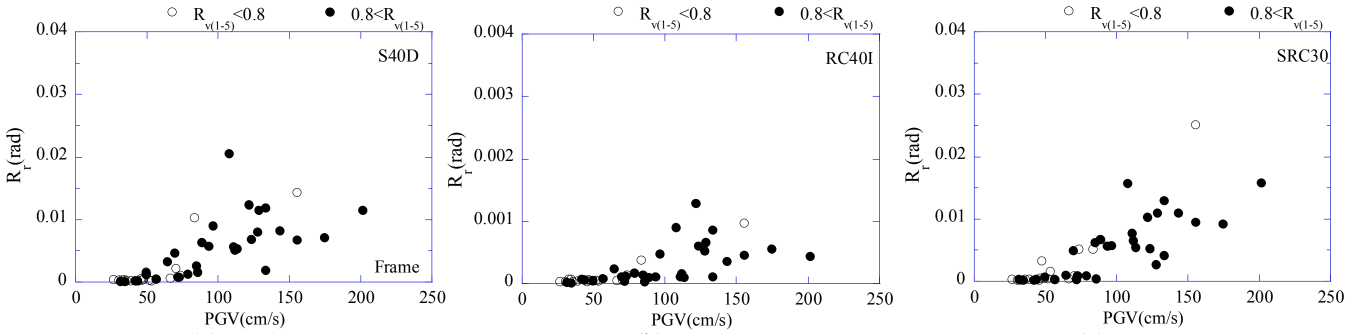

(a) S40D (b) RC40I (c) SRC30

Fig.9 Residual story drift angle

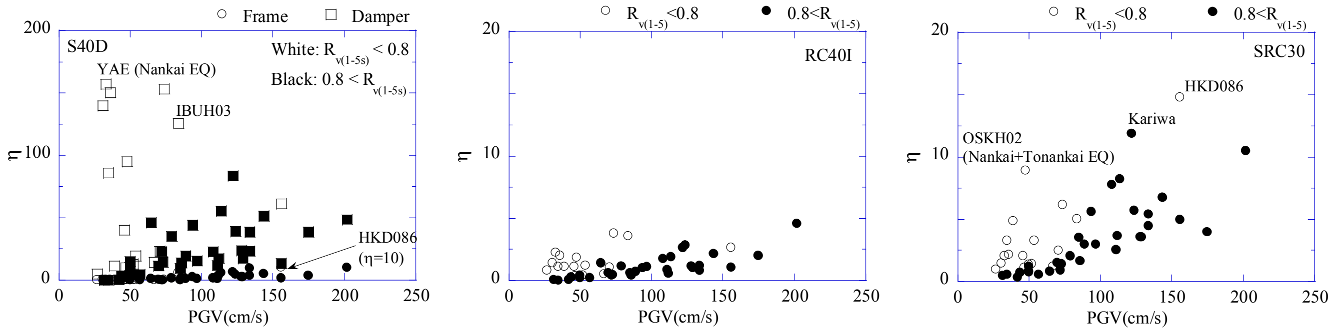

(a) S40D (b) RC40I (c) SRC30

Fig.10 Cumulative plastic deformation coefficient

The input motions of four earthquakes are assumed to be YAE (during 1995 Kobe EQ, Nankai EQ, Tonankai EQ, Nankai+Tonankai EQ (estimated by Turugi[4])), and KnkIkw (during Uemachi Faults (estimated by Active Fault Research Center Geological Survey of Japan[5]) , respectively. Cumulative damage D of buildings is estimated as follows, based on cumulative plastic ductility η.

$$D = (\eta_1 + \eta_2 + \eta_3 + \cdots)/\eta_u \tag{5.1}$$

In the present study, cumulative damage of S40D and SRC30 is estimated. The limit value of cumulative plastic ductility is set η_{uf} = 5 for frame, η_{ud} = 100 for damper. The followings can be pointed out from Table 4 and Figure 12.

a) The maximum drift angle for the KnkIkw during Uemachi Faults is about 0.02 and is much larger than that for the estimated Nankai earthquake or for the design motions specified in the Building Standard Law.

b) The cumulative plastic ductility and residual deformation for the four earthquakes are less than those for the HKD086 observed during the 2003 Off Tokachi Earthquake (Fig.10). Namely, the evaluation of ground motion is sometimes more important than the consideration of cumulative damage over in-service period.

Table 3 Earthquake occurrence scenario

Scenario No.	Event 1	Event 2	Event 3	Event 4
1	1995 Kobe EQ	Nankai EQ	Tonankai EQ	Uemachi Fault
2	1995 Kobe EQ	Nankai EQ + Tonankai EQ	Uemachi Fault	-
3	1995 Kobe EQ	Uemachi Fault	Nankai EQ	Tonankai EQ
4	1995 Kobe EQ	Uemachi Fault	Nankai EQ + Tonankai EQ	-

Table 4 Cumulative Damage

Scenario EQ	S40D								SRC30				
	Frame					Damper							
	R_{max}(rad)	R_r(rad)	η_f	η_{uf}	η_f/η_{uf}	η_f	η_{uf}	η_f/η_{uf}	R_{max}(rad)	R_r(rad)	η_f	η_{uf}	η_f/η_{uf}
1995 Kobe EQ (YAE)	0.005	0.000	0.020	5	0.004	9.3	100	0.093	0.003	0.000	0.545	5	0.109
Uemachi Fault	0.029	0.007	3.478	5	0.696	38.7	100	0.387	0.018	0.009	3.967	5	0.793
Nankai EQ	0.010	0.000	0.533	5	0.107	157.3	100	1.573	0.004	0.000	2.016	5	0.403
Tonankai EQ	0.008	0.000	0.003	5	0.001	19.5	100	0.195	0.012	0.001	3.257	5	0.651
Nankai + Tonankai EQ	0.012	0.001	0.405	5	0.081	153.4	100	1.534	0.015	0.005	6.124	5	1.225

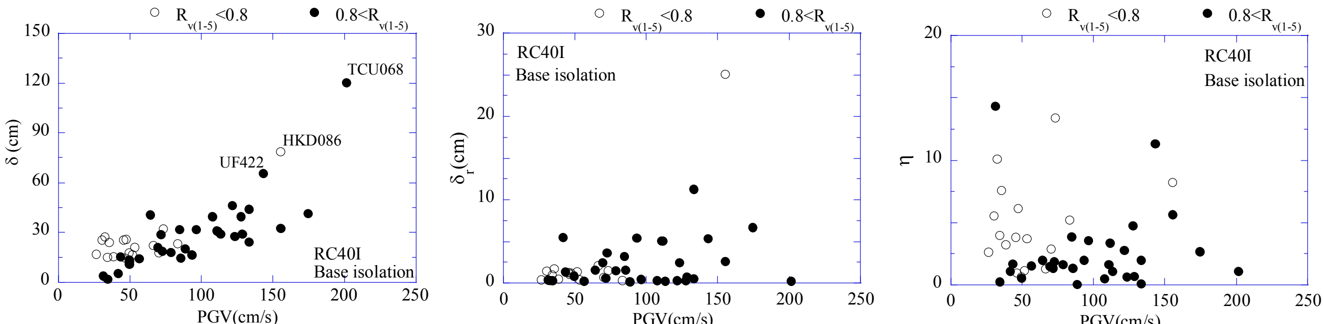

(a) Maximum drift deformation (b) Residual deformation (c) Cumulative plastic deformation coefficient

Fig.11 The maximum deformation of base isolation device (RC40I)

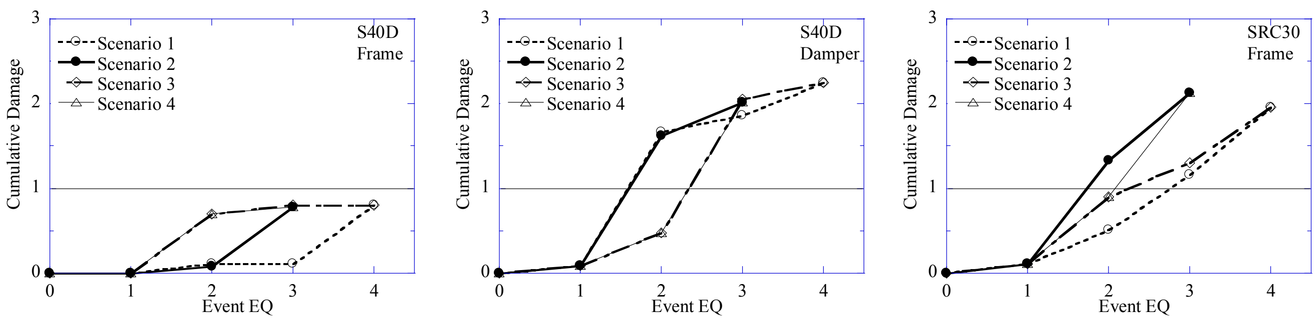

(a) S40D Frame (b) S40D Damper (c) SRC30

Fig.12 Cumulative damage over in-service period

6. CONCLUSIONS

In this paper, we characterize the remaining seismic performance of existing buildings and required performance for newly-built super-high-rise buildings in terms of the cumulative damage, such as the cumulative plastic deformation residual deformation, of the buildings during the in-service period. Ground motion simulations and observed ground motions strongly suggests that a long-period ground motion, especially of around 5 second components, would be amplified by the deep geological structure under Osaka basin during the earthquakes. We evaluated the cumulative damage of the three super-high-rise buildings in the Osaka basin during the in-service period. Our conclusions are as follows:

1) The characteristics of input motions and building responses can be successfully categorized by using a concept of impulse index corresponding to the ratio of the maximum instantaneous input energy to total input energy.
2) The cumulative residual drift and plastic displacement during the in-service period is not so large, while the maximum shear story drift angle may equal to or larger than 0.02.

ACKNOWLEDGEMENT

We used valuable seismic data recorded by the Japan Meteorological Agency, dataset of the K-NET and KiK-net operated by the National Research Institute for Earth Science and Disaster Prevention, and the seismic data recorded by, the Committee of earthquake observation and research in the Kansai Area.

REFERENCE

[1] The Headquarters for Earthquake Research Promotion : http://www.jishin.go.jp/main/index.html(in Japanese).
[2] Trifunac, M.D. and A.G. Brady: A study on the duration of strong earthquake ground motion, Bulletin of the Seismological Society of America, Vol.65, pp.581-626, 1975.
[3] Y.Inoue: The Outline of Simulated Earthquake Motion in Osaka City and Osaka Prefecture , The 31rd Symposium of Earthquake Ground Motion, pp.53-56, 2003(in Japanese).
[4] M.Turugi ，Boming Zhao，Petukhin Anatoly，Takao Kagawa : Strong ground motion prediction during the Nankai and Tonankai Earthquake in Osaka Prefecture，Journal of Structual Engineering，Vol.51A，pp.501-512， 2005.3(in Japanese).
[5] Active Fault Research Center Geological Survey of Japan: Report Earthquake Ground Motions Map around Osaka Prefecture - Research Report of Estimated Earthquake Ground Motions Provisional Edition -, 2005 (in Japanese).
[6] The Central Disaster Prevention Council, Cabinet Office, Government of Japan : The Commission of Experts of Tonankai and Nankai Earthquake, http://www.bousai.go.jp/jishin/chubou/nankai/index_chukin.html.